Generalization and propagation of spiraling Bessel beams with a helical axicon*

Sun Qiong-Ge(孙琼阁)[a], Zhou Ke-Ya (周可雅)[a], Fang Guang-Yu (方光宇)[a], Liu Zheng-Jun(刘正君)[b], and Liu Shu-Tian (刘树田)[a]†

[a] *Department of physics, Harbin Institute of Technology, Harbin 150001, China*

[b] *Department of Automation Measurement and Control Engineering, Harbin Institute of Technology, Harbin 150001, China*

(Received 25 July 2011; revised manuscript received 24 August 2011)

A generalized type of spiral Bessel beam has been demonstrated by using a spatially displaced helical axicon (HA). The topological charge of the spiraling Bessel beams is determined by the order of the input Laguerre–Gaussian (LG) beam and the topological charge of the HA. The obtained spiraling Bessel beams have an LG type of modulation along their propagation direction and exhibit annihilation-reconstruction properties. Theoretical analysis is presented, including that of the stability, propagation distance, topological charge, and spiraling dynamic characteristics. The mathematical and numerical results show that the propagation distance and helical revolution of the spiraling Bessel beams can be controlled through choosing appropriate radius of the HA.

Keywords: Bessel beam, helical axicon, beam propagation, spiral beam

PACS: 42.60.Jf, 42.40.Eq, 42.25.Bs **DOI:** 10.1088/1674-1056/21/1/014208

1. Introduction

Optical waves with special propagation characteristics have always received a great deal of interest. In 1987, Durnin introduced a novel class of exact solutions of the free space scalar wave equation, which is known as the zero-order Bessel beam.[1] Subsequently, a good approximation to such a beam is experimentally developed by the same group,[2] and extensive research has been made due to its non-diffracting and self-reconstructive characteristics.[3−6] Afterwards, more efficient methods to generate the Bessel beams have been proposed.[7−14] For example, the zero-order Bessel beam can be successfully generated with an axicon.[13] High-order Bessel beams can also be generated by an apertured axicon illuminated with a single-ringed Laguerre–Gaussian (LG) mode.[14] One common feature of the above-mentioned methods is that the output high-order Bessel beams have the same value of the topological charge as that of the input LG mode. However, with a helical axicon (HA), which is fabricated by the photolithographic process and regarded as the hybrid of an axicon and a spiral phase plate, the high order Bessel beams of desired topological charges can be generated.[15−20] Recently, optical beams that rotate around the optical axis are widely investigated.[21−24] One type of these beams keeps its transverse intensity distribution pattern invariant on propagation with scaled-rotating along the propagation.[25,26] Another type of these beams, which is referred to as helicon beams, has an intensity pattern which rotates at a constant rate about the optical axis, but is otherwise unchanged.[27−30] All these special rotating beams can be generated by using diffractive optical element (DOE).[31−33] Among the helicon beams, one special kind called the spiraling Bessel beam is recently proposed, whose intensity pattern can rotate about the optic axis as a whole and which keep its intensity scale unchanged upon propagation.[34−36] However, the above mentioned high-order spiraling beams have the same value of the topological charge as that of the input beam, which has been restricted to the single-ringed LG mode.

In this article, we propose a method to transform the LG beams into a generalized spiraling Bessel beam

*Project supported by the National Basic Research Program of China (Grant No. 2011CB301801), the National Natural Science Foundation of China (Grant Nos. 10974039, 11047153, 10904027, 61008039, and 11104049), the Doctoral Program of Higher Education of China (Grant No. 20102302120009), and the Fundamental Research Funds for the Central Universities of China (Grant No.2009038).

†Corresponding author. E-mail: stliu@hit.edu.cn

© 2012 Chinese Physical Society and IOP Publishing Ltd

with adjustable orders by a specially designed HA. The order of the spiraling output beams is determined not only by the input LG beams, but also by the topological charge of the HA. The change of the value and sign of the topological charge of generated spiraling Bessel beams also depends on the input LG beams and the HA. Under the given helical radius and helical pitch, we can obtain the wanted propagation distance and helical revolution which maintain the Bessel form by selecting an appropriate radius of the HA. In some special transverse planes, the spiraling beams near the axis will temporarily disappear and reconstruct themselves. The theoretical analysis of stability, propagation distance, topological charge, and spiraling dynamic characteristics is presented. The particular feature of spiraling Bessel beams makes them potentially useful for applications such as micro-fabrication, cold atom guiding, trapping, and rotating. [37−46]

2. Generation of spiraling Bessel beams with adjustable order

2.1. The design of the HA

In the thin transparency approximation, the transmission function of HA with integer topological charge p and lateral radius ρ is given by[15,20]

$$T(\rho,\varphi)=\exp(-\mathrm{i}\beta\rho+\mathrm{i}p\varphi), \tag{1}$$

where $\beta=k\gamma$, k is the wave number, $\gamma\approx(n_{\mathrm{r}}-1)\alpha$ is the angle of the deflected plane waves beyond the HA, α is the base angle and n_{r} is the material refractive index. In the polar coordinates, supposing the HA is displaced by a small displacement Δ from the optical axis, to the point $(\Delta\cos\psi,\Delta\sin\psi)$, the transfer function is changed according to

$$\begin{aligned}&T_{\Delta,\psi}(\rho,\varphi)\\&=\exp\{-\mathrm{i}\beta\left[\rho^2-2\Delta\rho\cos(\varphi-\psi)+\Delta^2\right]^{1/2}\\&\quad+\mathrm{i}p(\varphi-\phi)\},\end{aligned} \tag{2}$$

$$\phi=\arctan\frac{\Delta\sin(\psi-\varphi)}{\rho-\Delta\cos(\psi-\varphi)}. \tag{3}$$

Applying the Taylor expansion and taking the small displacement Δ into account, a simplified version of the transfer function is derived as

$$\begin{aligned}&T_{\Delta,\psi}(\rho,\varphi)\\&=\exp[-\mathrm{i}\beta\rho+\mathrm{i}p\varphi+\mathrm{i}\beta\Delta\cos(\varphi-\psi)].\end{aligned} \tag{4}$$

In order to obtain the regular spiraling output beams, we consider a special HA, which is divided into circular segments that are placed separately with the same helical radius Δ but a different polar angle $\psi_\Gamma=\Gamma\rho$ in the transverse plane. The HA with this special design will have the transfer function

$$\begin{aligned}&T_{\Delta,\Gamma}(\rho,\varphi)\\&=\exp[-\mathrm{i}\beta\rho+\mathrm{i}p\varphi+\mathrm{i}\beta\Delta\cos(\varphi-\Gamma\rho)].\end{aligned} \tag{5}$$

The helical period is defined by $P=2\pi/\Gamma$. Equation (5) can be regarded as the combinative transfer functions of the generic HA and a hologram $T_{\mathrm{H}}(\rho,\varphi)=\exp[\mathrm{i}\beta\Delta\cos(\varphi-\Gamma\rho)]$, or an axicon $T_\rho(\rho)=\exp(-\mathrm{i}\beta\rho)$ with a spiral phase plate (SPP) $T_\varphi(\varphi)=\exp(\mathrm{i}p\varphi)$ and a hologram. The hologram can be realized by a spatial light modulator.

2.2. The generation of spiraling Bessel beams with adjustable orders

Figure 1 shows a possible experimental setup which can generate the spiraling non-diffractive or diffractive Bessel beams. The first holographic element modulates a linearly polarized fundamental Gaussian mode to an LG mode. The spiraling non-diffractive beam is obtained when the DOE is placed at the waist ($\xi=0$) of the input beam, and the corresponding diffractive one will be obtained when $\xi\neq0$. For a much simpler and useful application, we consider the non-diffractive condition $\xi=0$. In the cylindrical coordinates, the field distribution of the mode is described as

$$\begin{aligned}E(\rho,\varphi)=&\left(\frac{2\rho^2}{\omega_0^2}\right)^{|l|/2}L_n^{|l|}\left(\frac{2\rho^2}{\omega_0^2}\right)\\&\times\exp\left(-\frac{\rho^2}{\omega_0^2}\right)\exp(\mathrm{i}l\varphi),\end{aligned} \tag{6}$$

where $L_n^{|l|}\left(2\rho^2/\omega_0^2\right)$ is the generalized Laguerre polynomial. The parameter n is a positive integer which determines the radial mode number, and l is an integer which expresses the optical vortex beam with topological charge $+l$ or $-l$, depending on the rotation direction of its helical wavefront. The transversal amplitude profile radius of the waist of input LG beams is expressed as $\eta_n^{|l|}=\omega_0\sqrt{2n+|l|+1}$.[20]

After placing the HA with radius of R at the waist of the incident beam, this radius will act as a beam truncation when $R<\eta_n^{|l|}$. The function is defined as

$$B(\rho)=\begin{cases}1 & \text{if } \chi\geq1,\\ \mathrm{circ}\left(\rho/\chi\eta_n^{|l|}\right) & \text{otherwise,}\end{cases} \tag{7}$$

with $\chi = R/\eta_n^{|l|}$. The field distribution behind the DOE can be described by using the Fresnel diffraction integral as

$$H(r,\psi,z) = \frac{1}{\mathrm{i}\lambda z}\exp\left[\mathrm{i}k\left(z+\frac{r^2}{2z}\right)\right] \times \int_0^R\int_0^{2\pi} B(\rho)H_0(\rho,\varphi)\exp\left(\frac{\mathrm{i}k\rho^2}{2z}\right) \times \exp\left(-\frac{\mathrm{i}kr\rho\cos(\psi-\varphi)}{z}\right)\rho\mathrm{d}\rho\mathrm{d}\varphi, \quad (8)$$

where H_0 can be written as

$$H_0(\rho,\varphi) = L(\rho)\exp\left(-\frac{\rho^2}{\omega_0^2}\right)\exp(\mathrm{i}\varphi l)T_{\Delta,\Gamma}(\rho,\varphi), \quad (9)$$

with

$$L(\rho) = \left(\frac{2\rho^2}{\omega_0^2}\right)^{|l|/2} L_n^{|l|}\left(\frac{2\rho^2}{\omega_0^2}\right). \quad (10)$$

From Eq.(8), we can obtain

$$H(r,\psi,z) = \frac{k}{2\pi\mathrm{i}z}\int_0^\infty B(\rho)\Omega(\rho)L(\rho) \times \exp\left[-\frac{\rho^2}{\omega_0^2}-\mathrm{i}\beta\rho+\frac{\mathrm{i}k}{2z}\left(r^2+\rho^2\right)\right]\rho\mathrm{d}\rho. \quad (11)$$

The integral

$$\Omega(\rho) = \int_0^{2\pi}\mathrm{d}\varphi\exp\left\{\mathrm{i}(p+l)\varphi+\mathrm{i}\left[\beta\Delta\cos(\varphi-\Gamma\rho) - \frac{kr\rho}{z}\cos(\varphi-\psi)\right]\right\} \quad (12)$$

can be further expressed as

$$\Omega(\rho) = (-\mathrm{i})^{l+p}2\pi A J_{l+p}(\sigma), \quad (13)$$

and

$$\sigma = \left[(\beta\Delta)^2+\left(\frac{kr\rho}{z}\right)^2 - 2\beta\Delta\frac{kr\rho}{z}\cos(\psi-\Gamma\rho)\right]^{1/2}, \quad (14)$$

$$A = \exp\left[\mathrm{i}(l+p)(\Gamma\rho-\Phi)\right], \quad (15)$$

$$\tan\Phi = \frac{\frac{kr\rho}{z}\sin(\Gamma\rho-\psi)}{\beta\Delta-\frac{kr\rho}{z}\cos(\Gamma\rho-\psi)}. \quad (16)$$

For a small displacement Δ, the integral in Eq. (11) can be evaluated approximately by the stationary phase method. The phase term of the expression under the integral is $\Psi = -\beta^2 z/2k + k(\rho - z\beta/k)^2\big/2z$. Solution to the equation of $\partial\Psi/\partial\rho \approx 0$ yields the critical point $\rho_\mathrm{c} = \gamma z$. The main contribution to the integral behaves as

$$H \propto \frac{(k\gamma\omega_0)^{1/2}}{\mathrm{i}^{l+p+1}}A_\mathrm{c}B(\rho_\mathrm{c})\left(\frac{\sqrt{2}z\gamma}{\omega_0}\right)^{|l|+1/2}L_n^{|l|}\left(\frac{2z^2\gamma^2}{\omega_0^2}\right) \times J_{l+p}(\sigma_\mathrm{c})\exp\left\{\mathrm{i}\left(\frac{kr^2}{2z}-\frac{\beta^2 z}{2k}\right)-\left(\frac{z\gamma}{\omega_0}\right)^2\right\}, \quad (17)$$

with $A_\mathrm{c} = A(\rho_\mathrm{c})$ and

$$\sigma_\mathrm{c} = \beta\left[\Delta^2+r^2-2r\Delta\cos(\psi-\Gamma z\gamma)\right]^{1/2}. \quad (18)$$

By neglecting the position-independent factors and satisfying the approximation of stationary phase method, then the intensity of the output field behind the DOE is approximately proportional to

$$I \propto k\,\gamma\,\omega_0\,I_n^{l+1/2}\left(z;\frac{\omega_0}{\gamma}\right)B^2(\rho_\mathrm{c})J_{l+p}^2(\sigma_\mathrm{c}), \quad (19)$$

where

$$I_n^{l+1/2}\left(z;\frac{\omega_0}{\gamma}\right) = \left(\frac{2z^2\gamma^2}{\omega_0^2}\right)^{|l|+1/2}\exp\left[-\frac{2z^2\gamma^2}{\omega_0^2}\right] \times\left[L_n^{|l|}\left(\frac{2z^2\gamma^2}{\omega_0^2}\right)\right]^2. \quad (20)$$

The stationary phase approximation requires that the region of the Bessel function is much larger than the width of the stationary phase region. This requirement leads to the proved condition $r^2 \le z\lambda/4$ under the condition of $\Delta = 0$,[14] and $r^2 \le z\lambda/\left[4+4(z\Gamma\gamma)^2\right]$ under the condition of $\Delta > 0$.[35] Therefore, the above derivative process shows its rationality and validity just under these two conditions.

Equation (19) reveals that spiraling Bessel-like beams with the order of $l+p$ rotate around the axis as they propagate, and the trajectory of the spiraling beams is determined by σ_c. An isocandela diagram of the generated spiraling Bessel beam of the first order is presented in Fig.1. We can see that the generated beam spirally propagates along the optic axis like a hollow spring.

From Eq. (20), the function $I_n^{l+1/2}(z,\omega_0/\gamma)$ is of the LG-doughnut type, which is related to the axial variable z instead of the radial variable r and has the half integer power in its definition, defining the longitudinal profile of spiraling Bessel beams. Therefore, we can conclude that the LG-doughnut type of function influences mainly the propagation distance of the spiraling beams which will be discussed in the following sections.

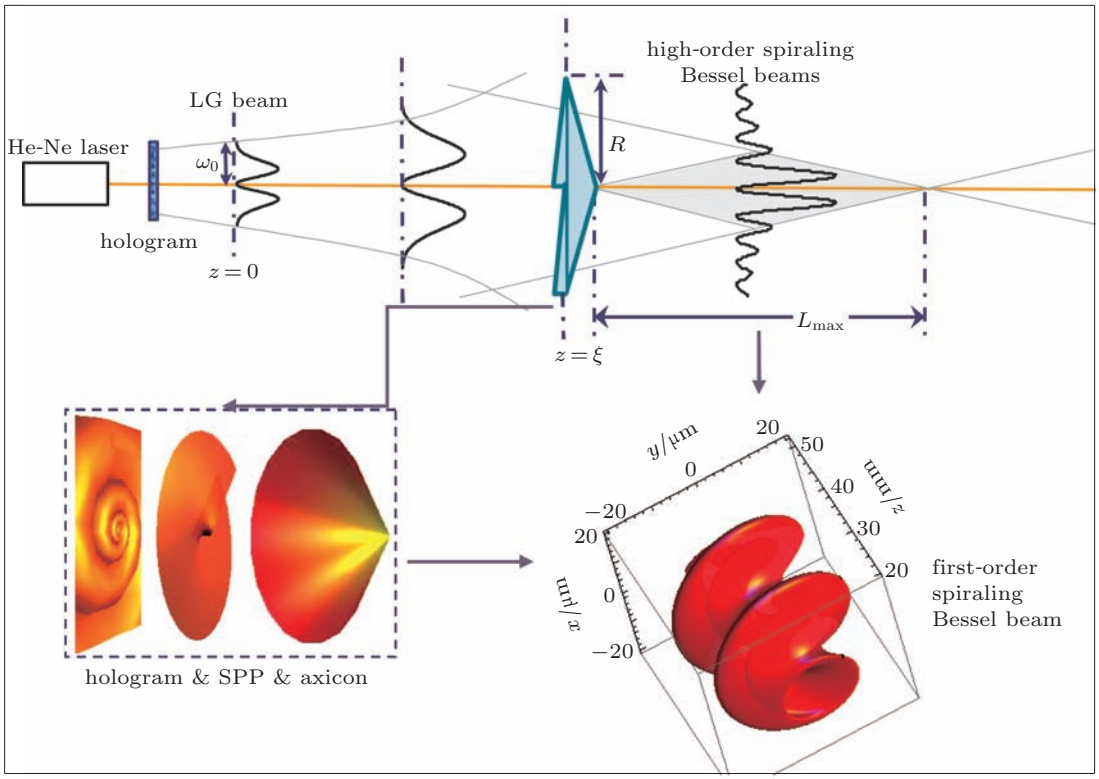


Fig. 1. A schematic illustration of the experimental setup for the generation of spiraling Bessel beams. A hologram and an HA are placed at the path of the LG mode. The first hologram serves as an element which generates an LG mode. The spiraling non-diffracting or diffracting Bessel beams can be observed in the shaded region with a characteristic length of $L_{\max}$. An isocandela diagram of the second-order spiraling Bessel beam is presented as an example, with $n=2$, $l=0$, $p=1$, $n_{\rm r}=1.5$, $\omega_0=2.5$ mm, $\alpha=4^\circ$, $P=0.5$ mm and $\Delta=10$ μm.

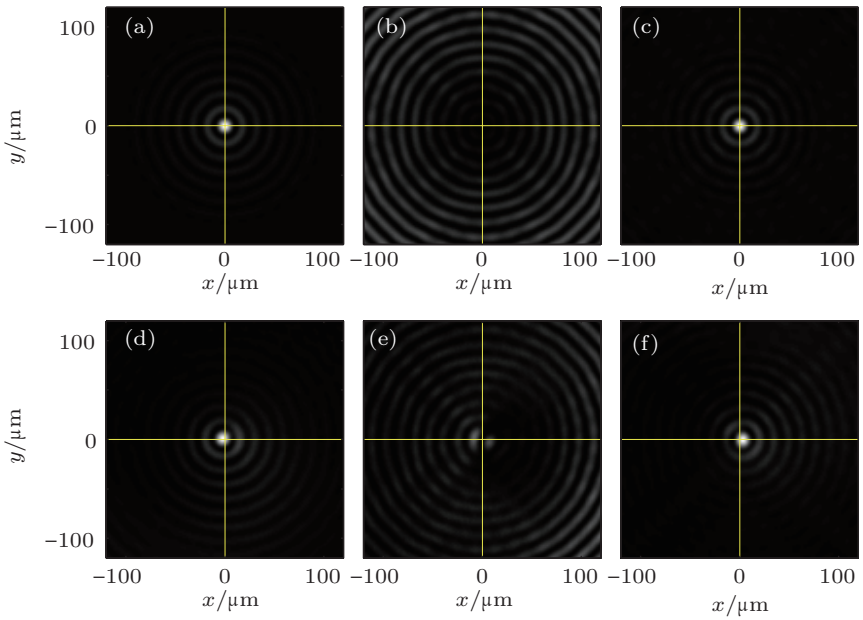


Fig. 2. (colour online) The self-reconstruction of the spiraling Bessel beams at different transverse sections. (a)–(c) When $\Delta=0$, the intensity distribution of Bessel beam at the distance of (a) $z=36$ mm, (b) $z=38$ mm and (c) $z=42$ mm respectively. (d)–(f) When $\Delta=2$ μm, the intensity distribution of the spiraling Bessel beam at the distance of (d) $z=36$ mm, (e) $z=38$ mm and (f) $z=42$ mm respectively. Parameters are $n_{\rm r}=1.5$, $\omega_0=2.5$ mm, $n=2$, $l=0$, $p=0$, $\alpha=4^\circ$, $P=0.5$ mm.

Moreover, for the reason that the generalized Laguerre polynomial has some longitudinal axial zeros, the transverse intensity distribution of the Bessel beams will also be affected, which brings about the axial minimum but abaxial maximum intensity distribution of transverse sections (see Figs. 2(b) and 2(e)). The central energy of this special transverse section diffracts to the region which deviates from the optic axis to ensure the conservation of energy.

After this special transverse section, the beam will self-reconstruct immediately and propagate in the Bessel form again. Figure 2 presents this self-reconstruction process of the spiraling Bessel beams during their propagation.

3. The spiraling characteristics of the generated beams

Usually, the azimuthal velocity of the generated spiraling beam is associated with the phase in the stationary phase approximation, $\delta\Psi/\delta z = 2\pi\gamma/P$.[34–36] One revolution covers a distance of $\partial\Psi = 2\pi$, which leads to a helical pitch of $H = 2\pi/\Gamma\gamma = P/\gamma$, depending on the parameters P and γ. The revolution of the spiraling beam is $N_{\rm b} = L_{\rm b}/H$ in the Bessel zone, which is dependent on the helical pitch H and the beam waist ω_0. The helical pitch and revolution are evidently all independent of the spiraling order l and p. This has been proved by the numerical simulation. In Figs. 3(a)–3(d), the first order of spiraling Bessel beam has the propagation distance 14.3 mm over one revolution. We present each quarter revolution of the first order Bessel beam on propagation. This beam indeed spirals about the optic axis with the same deviation away from the center in the transverse section. Figures 3(e)–3(h) show the first four orders of spiraling beams with the same revolution of 0.25 over the propagation distance of 3.575 mm. This means they all have the same azimuthal velocity, helical pitch, and helical radius. When we increase the order of spiraling beams, the diameter increases correspondingly. When $l + p = 3$, the diameter is nearly 40 μm. In the optical region, this size is comparable to the de Broglie wavelength of an ultra-cold ensemble of atoms. If we drilled a hole in the center of the HA and the hologram, the conversion from LG beams to spiraling Bessel beams can provide the prospect of guiding the atoms along the hollow region of the spiraling path which forms a long, purely optical atom waveguide.

Then, what is the difference of influence between the parameters l and p? Figure 4 presents two combinations in the first order spiraling Bessel beam, one is $l = 0$ and $p = 1$, the other is $l = 1$ and $p = 0$. We can see from the figure that these two conditions not only have the same azimuthal velocity and propagation distance in one revolution, but also the same intensity distribution which reveals that the output of spiraling Bessel beams depends on the sum of l and p instead of their individual values.

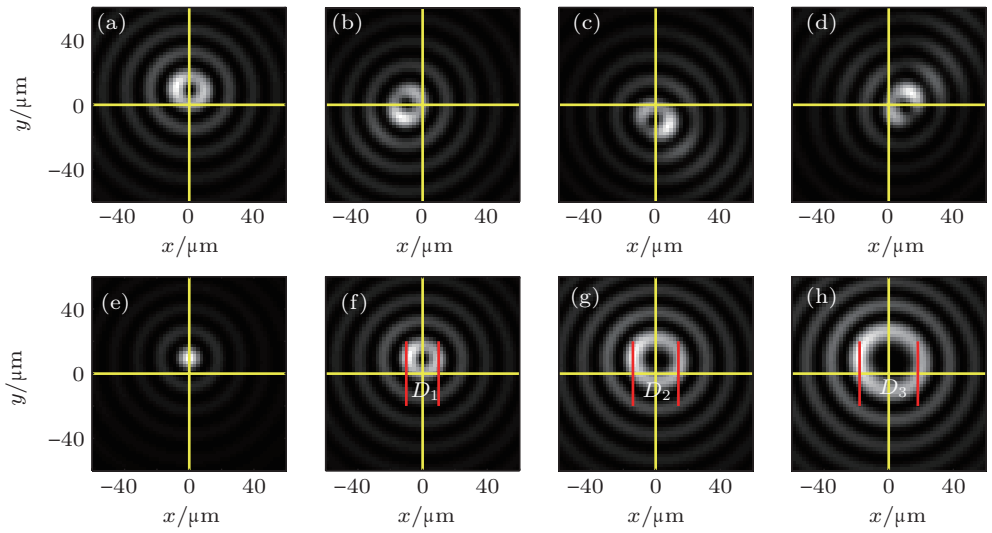


Fig. 3. (colour online) Intensity distribution of the spiraling Bessel beams at different transverse sections. (a)–(d) Order $l + p = 1$ propagates in one revolution with revolutions (a) $N = 0.25$, (b) $N = 0.5$, (c) $N = 0.75$, (d) $N = 1$. (e)–(h) Order $l = 0$ and (e) $p = 0$, (f) $p = 1$, (g) $p = 2$, (h) $p = 3$ at $z = 3.575$ with revolution $N = 0.25$. D_1, D_2, and D_3 are the diameters of the central hollow region. Parameters are $n_{\rm r} = 1.5$, $\omega_0 = 2.5$ mm, $n = 1$, $\alpha = 4°$, $P = 0.5$ mm, $\Delta = 10$ μm.

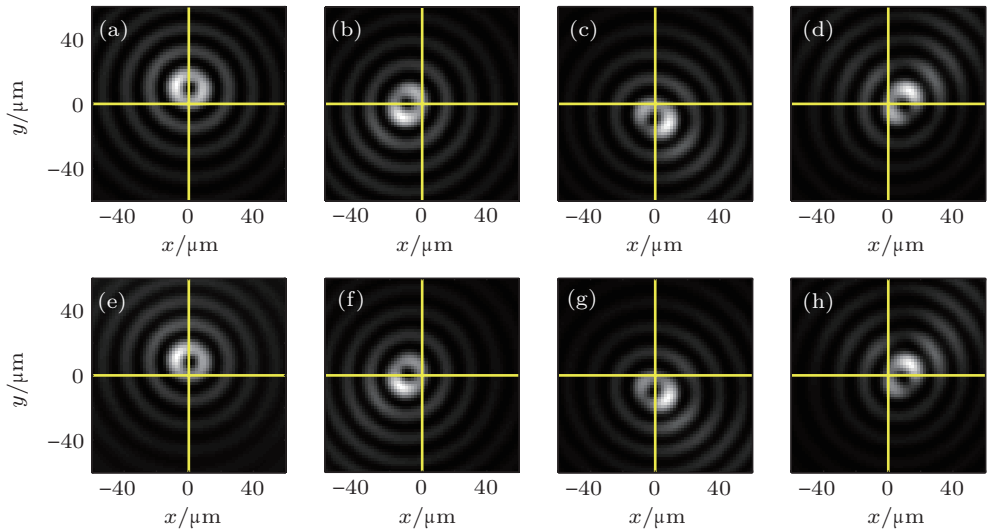


Fig. 4. (colour online) Intensity distribution of the spiraling Bessel beams in different transverse sections. (a)–(d) Order $l = 1$ and $p = 0$ at revolutions (a) $N = 0.25$, (b) $N = 0.5$, (c) $N = 0.75$, (d) $N = 1$. (e)–(h) Order $l = 0$ and $p = 1$ at revolutions (e) $N = 0.25$, (f) $N = 0.5$, (g) $N = 0.75$, (h) $N = 1$. Parameters are $n_{\rm r} = 1.5$, $\omega_0 = 2.5$ mm, $n = 1$, $\alpha = 4°$, $P = 0.5$ mm, $\Delta = 10$ μm.

4. The stability of the spiraling beams

The question remaining to be answered is the stability of the generated beams when the figure of the spiraling beams is perturbed. To solve these problems, similar to the conventional method, we define the form of the maximum helical radius of the generated beams as follows:

$$\Delta_{\rm m}^{(l+p)} = H\tau_{l+p}\left[\frac{z\lambda}{H^2+(2\pi z)^2}\right]^{1/2}, \qquad (21)$$

where $l+p$ stands for the sum of azimuthal mode numbers of incident beam and the topological charge of SPP, τ_{l+p} is the solution of the equation $J_{l+p}(2\tau_{l+p}) = \left|J_{l+p}\left(x_0^{(l+p+1)}\right)\right|$, and $x_0^{(l+p+1)}$ is the minimum positive root of the function $J_{l+p+1}\left(x_0^{(l+p+1)}\right) = 0$. The spiraling Bessel beams with adjustable orders and topological charge of $l+p$ maintain their Bessel profile as propagating about the axis under the condition $\Delta^{(l+p)} \leq \Delta_{\rm m}^{(l+p)}(z)$; otherwise, their Bessel profile will disappear.

As shown in Fig. 5(a), the maximum radius $\Delta_{\rm m}^{(l+p)}$ increases as the order increases except for zero order, because the shape of zero-order Bessel function differs from that of high-order Bessel functions. However, for a certain quantity of Δ, each order of spiraling beam has the same deviation from the propagation axis, and for a certain order of spiraling beam, it is also obvious that the spiraling beams' helical radius increases as Δ increases. Moreover, when we increase

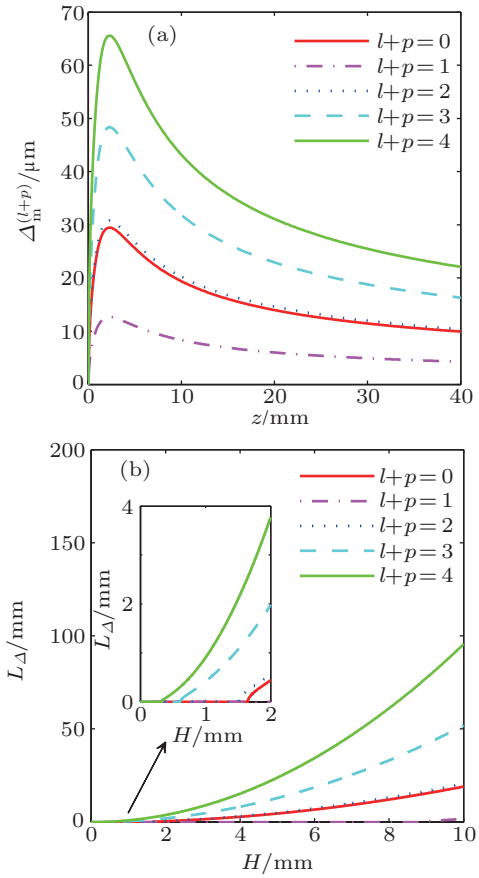


Fig. 5. (colour online) (a) The relation between the maximum allowable helical radius $\Delta_{\rm m}^{(l+p)}$ of the generated beams and the propagation distance with respect to the sum of topological charge of HA and azimuthal mode number. (b) For a given helical radius, the dependence of the critical helical pitch H on the value of propagation length L_Δ. Parameters are $n_{\rm r} = 1.5$, $\omega_0 = 2.5$ mm, $n = 1$, $\alpha = 4°$, $P = 0.5$ mm, $\Delta = 10$ μm.

the helical radius Δ, the profile of spiraling Bessel beams will be changed because of the stability. A numerical simulation has been presented to demonstrate the influence of the helical radius Δ on the spiraling beam and its stability. In Figs. 6(a)–6(d), when the helical radius is 2 μm, each order of Bessel beam can retain their profiles in an intact Bessel form, but in Figs. 6(e)–6(h), when the helical radius becomes 12 μm, the helical radius has a strong effect on the profile of each order of the beam. This means the helical radius is tightly associated with the stability of the output spiraling beam. In order to obtain the stable spiraling Bessel beams with desired propagation length, the maximum helical radius should be estimated first to ensure the stability. The quantity of Δ is dependent on the hologram, so the radius and stability of the spiraling Bessel beams can be modulated by the hologram which is generated by the spatial light modulator.

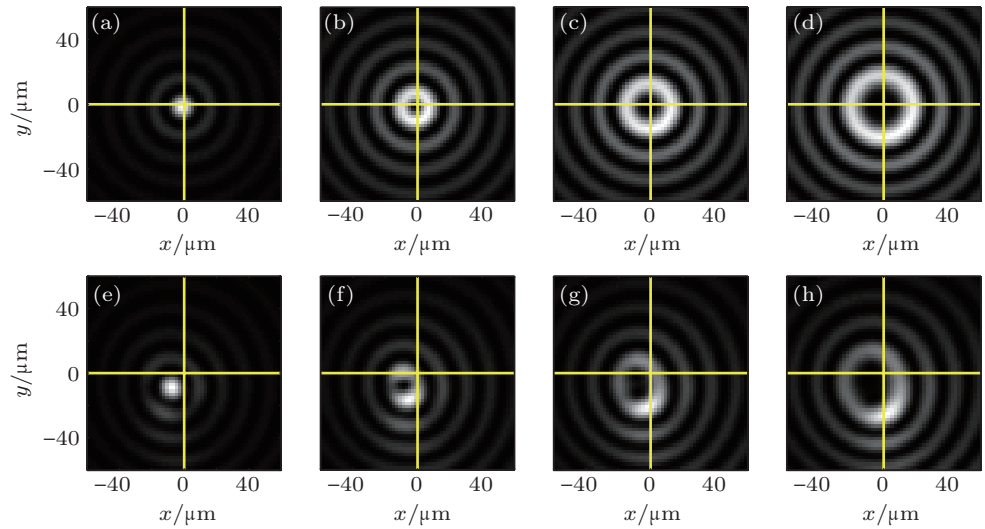


Fig. 6. (colour online) The influence of the helical radius Δ on the spiraling beams. (a)–(d) The first four orders of spiraling beams with $\Delta = 2$ μm. (e)–(h) The first four orders of spiraling beams with $\Delta = 12$ μm. (a), (e) $p = 0$; (b), (f) $p = 1$; (c), (g) $p = 2$; (d), (h) $p = 3$. The parameters are $n = 1$, $l = 0$, $p = 0$, 1, 2, 3, $N = 0.625$, $n_{\rm r} = 1.5$, $\omega_0 = 2.5$ mm, $\alpha = 4^\circ$, $P = 0.5$ mm.

5. The propagation distance of the spiraling beams

In order to find out the propagation distance of the outgoing spiraling Bessel beams, we study the distance of the non-spiraling Bessel beams first, which means that the HA is not specially designed. That is to say, let Δ equal zero. If we illuminate arbitrary LG beams to the HA, whose center is coincident with the optic axis at its waist $\xi = 0$, the output approximate intensity distribution of Bessel-like beams will be given by

$$I \propto k\ \gamma\ \omega_0\ I_n^{l+1/2}\left(z;\frac{\omega_0}{\gamma}\right) B^2\left(\rho_{\rm c}\right) J_{l+p}^2\left(kr\gamma\right) \quad (\Delta = 0), \tag{22}$$

where the critical point is still $\rho_{\rm c} = \gamma z$. The function $I_n^{l+1/2}\left(z, \omega_0/\gamma\right)$ is of the LG-doughnut type, which is related to the axial variable z instead of the radial variable r, and has the half integer power in its definition, defines the longitudinal profile of non-spiraling Bessel beams. First, when $\chi \leq 1$, the outgoing beams propagate within the distance $0 < z \leq \chi\eta_n^{|l|}/\gamma$, the propagation distance is

$$L_{\rm b} = \frac{\chi\omega_0}{\gamma}\sqrt{2n + |l| + 1} = \frac{R}{\gamma}, \tag{23}$$

which can be controlled by modulating the radius of HA. Second, when $\chi > 1$, the propagation distance is

$$L_{\rm b} = \frac{\omega_0}{\gamma}\sqrt{2n + |l + 1/2| + 1}, \tag{24}$$

which depends on the azimuthal and radial mode numbers of the input beam. For the special condition of $n = 0$, the theoretical analysis has been made in Ref. [20].

The non-spiraling Bessel beams have a dark core in the center except the order of $l + p = 0$. Its dark core is surrounded by a light ring of radius

$$r_{\max} = \mu_{l+p,1}/\beta, \tag{25}$$

where $r_{\max}$ is found as a root of the equation

$$\left|J_{|l+p|+1}\left(kr\gamma\right)\right| = \left|J_{|l+p|-1}\left(kr\gamma\right)\right|, \tag{26}$$

and $\mu_{l+p,1}$ is the first maximum defined by the first derivative of the Bessel function. Since the radius of non-spiraling Bessel beams in transverse section is independent of z, we can affirm that the outgoing beams are non-diffracting. The diffractive Bessel beams will be obtained conventionally under the condition $\xi \neq 0$.

Now, we will discuss the propagation distance of generated spiraling beams with adjustable orders and topological charges. For a given helical radius Δ, the propagation length of generated beams is

$$L_\Delta = \frac{H}{\pi}\left[\left(\frac{\tau_{l+p}}{\Delta}\right)^4\left(\frac{\lambda H}{4\pi}\right)^2 - 1\right]^{1/2}. \tag{27}$$

Obviously, the propagation length of the output beam is strictly dependent on the helical pitch H and the sum of the azimuthal mode number of the input beam and the topological charge of HA, and this relationship has been presented in Fig. 5(b). The solution of Eq. (27) is the critical helical pitch $H_{\rm L}$. Under a given propagation length L, the $H_{\rm L}$ increases as the order increases except for zero order. The value of $H_{\rm L}$ must achieve a suitable quantity to ensure the high order beams' propagation, otherwise the generated beams will not propagate in the spiraling way with the intact Bessel profile. Under this critical helical pitch, the propagation length of each order increases as the helical pitch H increases. The number of revolutions over this length is $N_\Delta = L_\Delta/H$.

For the given spiraling radius Δ and helical pitch H, the real propagation length of spiraling beams is dependent on the minimum of the spiraling propagation length L_Δ and the Bessel zone $L_{\rm b}$. If $L_\Delta < L_{\rm b}$, the real propagating length is L_Δ and the real revolution is N_Δ. If $L_\Delta > L_{\rm b}$, the real propagating length is $L_{\rm b}$ and the real revolution is $N_{\rm b}$. Exceeding the minimum of $\{L_\Delta, L_{\rm b}\}$, the spiraling high-order Bessel beams do not propagate with the Bessel profile in a spiraling way.

For example, we adopt the (2, 1) mode for the incident beam, the topological charge of the HA is $p = 1$. First, when $\chi > 1$, we may expect $N_{\rm b} \approx 12$ revolutions per Bessel zone. However, because of the restriction in Eq. (28) which is obtained from the stationary phase method, the actual number of revolutions is $N_\Delta \approx 3$. This condition is presented in Fig. 7. The figure shows that the profile of spiraling Bessel beams gradually deforms as they spiral about the optic axis. The generated Bessel beam can no longer keep its profile when the number of revolutions exceeds three. Second, when $\chi \leq 1$, we may expect the revolution number $N_{\rm b} = R/P$, and the radius R serves as a modulation parameter to handle the propagation length. If $L_{\rm b} = R/\gamma \leq L_\Delta$, the real revolution number is dependent on $N_{\rm b}$; on the contrary, the real revolution number will be N_Δ, but we can always select a proper R to ensure $L_{\rm b} \leq L_\Delta$. In conclusion, no matter whether $\chi > 1$ or $\chi \leq 1$, the desired propagation length can be gained by selecting the proper radius of HA. Furthermore, the other special conditions have been presented in other articles. When $p = 0$, $l = 0$ and $n = 0$, the output will be a zero order spiraling Bessel beam which was described in Ref. [35].

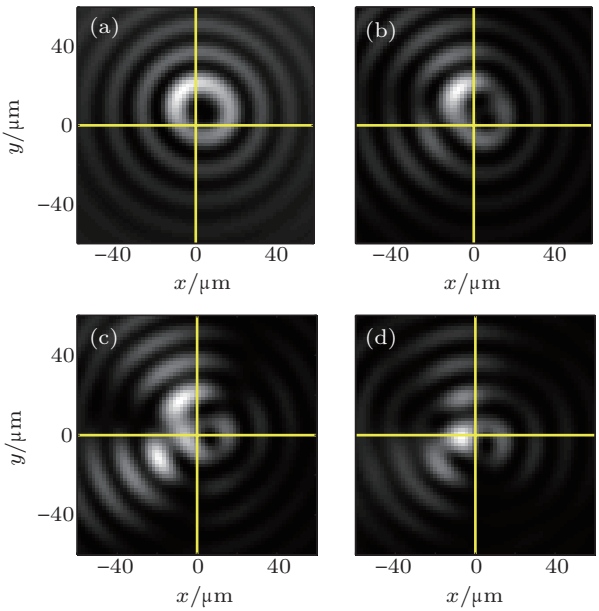


Fig. 7. (colour online) The stability of the second-order spiraling Bessel beams in different transverse sections with the revolutions (a) $N = 0.2$, (b) $N = 1.2$, (c) $N = 2.2$, and (d) $N = 3.2$. Parameters are $n = 2$, $l = 1$, $p = 1$, $n_{\rm r} = 1.5$, $\omega_0 = 2.5$ mm, $\alpha = 4°$, $P = 0.5$ mm, $\Delta = 10$ μm.

6. The topological charge of the generated beams

For convenience, we take the positive azimuthal mode number l ($l > 0$). For both cases of $\chi \leq 1$ and $\chi > 1$, the sign of $l + p$ determines the rotation direction of the wavefront. Moreover, the output beams have a phase singularity along the spiraling propagation path and carry a topological charge of $|l + p|$. Their vortex core is surrounded by coaxial bright and dark rings, except for the case of l and p having equal values but opposite signs ($|l + p| = 0$) which presents the spiraling zero order Bessel beam.

For the first condition of positive p, the output

spiraling Bessel beams have the increased topological charge of $l+p$ and vortex radius compared with that of the incident LG beams. When $-l < p < 0$, the output spiraling Bessel beams have the decreased topological charge $l - p$ and vortex radius instead. If $p = -l$, the phase singularity of the incident LG beams annihilates with that of the hologram HA, and the zero order spiraling Bessel beam whose intensity distribution has a bright central spot will be generated. When $p < -l$, the output spiraling Bessel beams have topological charge of $|l - p|$ and the opposite rotation direction of wavefront compared with the incident LG beams.

The condition of $p = 0$ means that only a specially designed axicon is present instead of the specially designed HA. The intensity distribution of the outgoing beams behind the DOE represents the spiraling Bessel beam of the lth order, the topological charge of the outgoing beams is the same as that of the incident beam. The condition of $l = 0$ and $n = 0$, which means the input optic field is of a Gaussian distribution, generates the diffracted wave field expressed as a spiraling vortex beam of p order, and the value of p depends on the SPP.

7. Conclusion

In conclusion, we have proved theoretically the transformation of the LG beams into spiraling Bessel beams which has adjustable topological charges compared with the incident LG beams. The order and topological charge of the generated spiraling beams not only depends on the incident LG beams but also on the topological charge of the HA. The helicity of the wavefront of the generated spiraling beams can be changed according to the alteration of the sign of $l + p$. We provide a new way to generate conventional high order or zero order spiraling beam by the use of the HA, and offer a method to increase or decrease the topological charge, change the rotation direction of the wavefront of the generated spiraling beams. Especially, when the helical radius Δ equals zero, Bessel beams can be generated from arbitrary LG beams instead of the single-ringed LG beam. Moreover, the spiraling beams will temporarily disappear as a special place near the axis and self-reconstruct immediately. Theoretical analysis for the stability, propagation distance, topological charge, and spiraling dynamic characteristics has been presented. In our numerical simulation, one can draw the following three remarks: firstly, the shape of spiraling trajectory can be modulated by the helical radius Δ and the helical pitch H, which makes it possible to control the output spiraling Bessel beams through modulating the hologram. Secondly, by choosing a proper HA and the input LG beams, the desired topological charge and the helicity of the wavefront of the output beams can be controlled. Thirdly, the desired propagation distance and helical revolution can be modulated simply by selecting the appropriate radius of HA.

Spiraling Bessel beams have potential applications in micro fabrication, especially for cold atom guiding due to their inherent characteristics. If a hole is drilled in the center of the combination of HA and hologram, the ultra-cold atom can be guided to utilize the innate "hollow" center of the high order Bessel beams, which can be viewed as a purely optical guide.

References

[1] Durnin J 1987 *J. Opt. Soc. Am.* A **4** 651
[2] Durnin J and Miceli J J 1987 *Phys. Rev. Lett.* **58** 1499
[3] Bouchal Z, Wagner J and Chlup M 1998 *Opt. Commun.* **151** 207
[4] Jarutis V, Paškauskas R and Stabinis A 2000 *Opt. Commun.* **184** 105
[5] Litvin I A, Mclaren M G and Forbes A 2009 *Opt. Commun.* **282** 1078
[6] Belyi V, Forbes A, Kazak N, Khilo N and Ropot P 2010 *Opt. Express* **18** 1966
[7] Phelan C F, O'Dwyer D P, Rakovich Y P, Donegan J F and Lunney J G 2009 *Opt. Express* **17** 12891
[8] Litvin I A, KhiloN A, Forbes A and Belyi V N 2010 *Opt. Express* **18** 4701
[9] Carbajal-Dominguez A, Bernal J, Martin-Ruiz A and Gabriel M N 2010 *Opt. Express* **18** 8400
[10] Rosen J, Salik B and Yariv A 1995 *J. Opt. Soc. Am.* A **12** 2446
[11] Jarutis V, Matijošius A, Smilgevičius V and Stabinis A 2000 *Opt. Commun.* **185** 159
[12] Paterson C and Smith R 1996 *Opt. Commun.* **124** 121
[13] Herman R M and Wiggins T A 1991 *J. Opt. Soc. Am.* A **8** 932
[14] Arlt J and Dholakia K 2000 *Opt. Commun.* **177** 297
[15] Khonina S N, Kotlyar V V, Soifer V A, Shinkaryev M V and Uspleniev G V 1992 *Opt. Commun.* **91** 158
[16] Khonina S N, Kotlyar V V, Shinkaryev M V, Soifer V A and Uspleniev G V 1992 *J. Mod. Opt.* **39** 1147
[17] Beijersbergen M W, Coerwinkel R P C, Kristensen M and Woerdman J P 1994 *Opt. Commun.* **112** 321
[18] Kotlyar V V, Almazov A A, Khonina S N, Soifer V A, Elfstrom H and Turunen J 2005 *J. Opt. Soc. Am.* A **22** 849
[19] Kotlyar V V, Kovalev A A, Skidanov R V, Moiseev O Y and Soifer V A 2007 *J. Opt. Soc. Am.* A **24** 1955
[20] Topuzoski S and Janicijevic L 2009 *Opt. Commun.* **282** 3426
[21] Abramochkin E G and Volostnikov V G 1993 *Opt. Commun.* **102** 336
[22] Abramochkin E G and Volostnikov V G 1996 *Opt. Commun.* **125** 302

[23] Abramochkin E G and Volostnikov V G 2004 *Phys. Usp.* **174** 1177

[24] Izdebskaya Y, Shvedov V and Volyar A 2008 *J. Opt. Soc. Am.* A **25** 171

[25] Schechner Y Y, Piestun R and Shamir J 1996 *Phys. Rev. E* **54** R50

[26] Kotlyar V V, Soifer V A and Khonina S N 1997 *J. Mod. Opt.* **44** 1409

[27] Paterson C and Smith R 1996 *Opt. Commun.* **124** 131

[28] Alonzo C A, Rogrigo P J and Glückstad J 2005 *Opt. Express* **13** 1749

[29] Bentley J B, Davis J A, Bandres M A and Gutiérrez-Vega J C 2006 *Opt. Lett.* **31** 649

[30] Alonzo C A, Rodrigo P J and Glückstad J 2005 *Opt. Express* **13** 1749

[31] Piestun R, Spector B and Shamir J 1996 *J. Opt. Soc. Am.* A **13** 1837

[32] Zhang B and Zhao D 2010 *Opt. Express* **18** 12818

[33] Vasara A, Turunen J and Friberg A T 1989 *J. Opt. Soc. Am.* A **6** 1748

[34] Matijošius A, Jarutis V and Piskarskas A 2010 *Opt. Express* **18** 8767

[35] Jarutis V, Matijošius A, Trapan P D and Piskarskas A 2009 *Opt. Lett.* **34** 2129

[36] Sun Q, Zhou K, Fang G, Liu Z and Liu S 2011 *Appl. Phys.* B **104** 215

[37] Gustav S, Ralf N, Bilal Ö and Thomas W 2010 *Opt. Express* **18** 4510

[38] Mei Z and Zhao D 2005 *J. Opt. Soc. Am.* A **22** 1898

[39] Xie Q and Zhao D 2007 *Opt. Commun.* **275** 394

[40] Arlt J, Garces-Chavez V, Sibbett W and Dholakia K 2001 *Opt. Commun.* **197** 239

[41] Chávez-Cerda S, McDonald G S and New G H C 1996 *Opt. Commun.* **123** 225

[42] Orlov S, Regelskis K, Smilgevičius V and Stabinis A 2002 *Opt. Commun.* **209** 155

[43] Mcgloin D and Dholakia K 2005 *Contemporary Phys.* **46** 15

[44] He H, Heckenberg N R and Rubinsztein-Dunlop H 1995 *J. Mod. Opt.* **42** 217

[45] Shvedov V G, Rode A V, Izdebskaya Y V, Desyatnikov A S, Krolikowski W and Kivshar Y S 2010 *Opt. Photon. News* **21** 37

[46] Lin J, Yuan X C, Tao S H, Peng X and Niu H B 2005 *Opt. Express* **13** 3862